Journal of Thermal Analysis and Calorimetry, Vol. 95 (2009) 1, 31–36

STRUCTURAL ANALYSIS OF REACTIVE DYE SPECIES RETAINED BY THE BASIC ALUMINA SURFACE

A. Tabak[*]

Department of Chemistry, Faculty of Arts and Sciences, Rize University, 53100 Rize, Turkey

The alumina–dye composites were prepared by treating the basic alumina with the water solutions of Reactive Red 120 (RR 120) and Reactive Blue 15 (RB 15) dyes. The bands of low intensities in the 1400–1600 cm^{-1} region and at 783 cm^{-1} in the IR spectra of these composites point out that the dye species is bound weakly to the surface. In the case of mechanochemical adsorption of dye molecules, the asymmetric and symmetric $S(=O)_2$ and the S–O–C stretching bands together with the vibrations of aromatic ring revealed that dye types under dry conditions interacted effectively with alumina surface. After the heating of the alumina dye complexes in the temperature range 150–350°C, the intensities of the IR and XRD peaks for adsorbed types decreased. The endothermic peaks over 200°C and the bigger total mass losses for the alumina–dye composites can be ascribed to the decomposition of dye species retained by the alumina surface. The mass losses on TG curves of the alumina–dye complexes up to ~800°C exhibit the removal of black residues occurred by decomposition of first adsorbed products. The thermal analysis data also point out that the water molecules bonded strongly to the alumina surface and dye types compete to accommodate at the surface active sites.

Keywords: *alumina, FTIR, Reactive Blue 15, Reactive Red 120, TG-DTG-DTA, water bridge, XRD*

Introduction

Aluminas have been extensively used as filler, adsorbent, catalyst, drying agent due to their low cost and active surface structures [1–7]. Alumina oxides, especially, used in the chromatographic purification can be classified as basic, neutral and acidic types. Basic alumina is composed of ϒ-alumina and δ-alumina phases and its solution in the water yields a basic solution [8]. ϒ-alumina generally occurs through dehydration of gibbsite (ϒ-$Al(OH)_3$) or boehmite (ϒ-AlOOH) and the crystallisation of amorphous Al_2O_3. In the case of thermal dehydration of these materials, the thermodynamically stable (α) and intermediate aluminium phases (ϒ, δ, θ, κ, χ) at different temperatures are formed and also these products possess different physical properties depending on heating rate and calcination conditions [9]. For example, when the gibbsite is hydrothermally heated at 150°C, the boehmite occurs and the same product can be heated to form ϒ-Al_2O_3 in atmosphere at 300–450°C.

The alumina surface, on which are the OH^-, O^{2-} and Al^{3+} species, has both acidic and basic sites of varying strengths and concentration to impart the amphoteric property [10, 11]. The co-ordinately unsaturated Al^{3+} and OH^- ions on the surface form the Lewis and Brønsted acid sites while the basic sites occur in the presence of the O^{2-} and OH^- species [12].

The alumina surface is negatively charged at pH values greater than its isoelectric point due to the deprotonation of the surface hydroxyl groups, whereas the same surface is uncharged at its zero point of charge (ZPC) [13]. However, when alumina oxide is brought into contact with acidic aqueous solution, the surface carries a net positive charge because of protonation of the surface hydroxyl groups. Consequently, the adsorption of various molecules and occurrence of organic reactions on the alumina are closely related to surface properties [14–16].

The alumina oxide crystals can adsorb water molecules physically and chemically to minimize surface energy when exposed to moisture at room temperature. When alumina is heated at lower temperature, physisorbed H_2O is desorbed initially and then some reacts to form hydroxyl groups [17]. At higher temperatures, these groups and chemisorbed water are driven from the surface to impart active sites.

The interactions between some organic compounds and the alumina showed that the basic and acidic sites (Lewis and Brønsted) on the surface have influence on the adsorptive and catalytic properties of the alumina [12, 18, 19]. The nature, number and strength of these sites not only play an important role in many organic reactions but also give useful information about the interaction type among these species. In the case of reactive dyes including a reactive group such as vinyl sulphone, chlorotriazine, etc., the most of these dyes are azo or metal complex azo compounds and these molecules may also interact with the surface of alumina [20, 21]. The investigation of the thermal behaviours and spectroscopic properties of the dye-alumina composites can clarify the thermal

* ahmtabak@hotmail.com

1388–6150/$20.00
© 2008 Akadémiai Kiadó, Budapest
Akadémiai Kiadó, Budapest, Hungary
Springer, Dordrecht, The Netherlands

stabilities of these species and the nature of interaction on the active sites of the surface. This information is especially very important in solving environmental problems because the release of these dyes, which have the lower degree of fixation due to hydrolysis of reactive groups in the water phase, into the environment is undesirable.

The main objective of this research is to investigate the nature of interaction of the Reactive Red 120 (RR 120) and Reactive Blue 15 (RB 15) by basic alumina and the thermal stabilities by using X-ray diffraction (XRD), thermal analysis (DTA, TG and DTG) and Fourier Transform Infrared Spectroscopy (FTIR) techniques.

Experimental

Materials and methods

The basic alumina was purchased from Merck and the pH of it in water at 25°C was detected about 9.0±0.2. The chemical formula of RR 120 (Merck) and RB 15 (Sigma) dyes used in this study were presented in Figs 1a and b. All the chemicals are of analytical grade and used as received without further purification.

Adsorption experiments on the alumina were carried out in a batch process. 100 mg of alumina and 50 mL of aqueous $5 \cdot 10^{-5}$ M solutions of each dye were put into polyethylene tubes and shaken rigorously at 25°C. Adsorption studies demonstrated that the equilibrium of adsorption was reached in 36 h. The pH value subsequent to the addition of both dye solution to the alumina was recorded about 9.0±0.2 and the pH parameter was kept constant during the adsorption. At the end of the adsorption period, the suspensions were centrifuged for 5 min at 6.000 rpm and the solid phases were filtered, freeze-dried and then heated from room temperature to 350°C stepwise. The dye concentrations retained by the alumina were determined by the data from UV2 UV-VIS spectrophotometer.

Mechanochemical adsorptions of RR 120 and RB 15 dye compounds by alumina were carried out under dry conditions. The mixtures of dried alumina and dye species in the ratio of 6:10 were manually ground with an agate mortar and pestle for a few minutes at room temperature.

FTIR spectra of the alumina–dye composites were recorded in the region 4000–200 cm^{-1} on a Mattson-1000 FTIR spectrometer at a resolution of 4 cm^{-1}. XRD patterns were taken on a Rigaku 2000 automated diffractometer using Ni filtered CuK_α radiation. The TG, DTG and DTA curves were obtained using a PRIS Diamond TG/DTA (DSC) apparatus in a dynamic nitrogen atmosphere (heating rate: 10°C min^{-1}, platinum crucibles, mass ~10 mg and temperature range 25–1000°C).

Results and discussion

Shown in Fig. 2A (curves a–i) are the comparative FTIR spectra of untreated alumina and the alumina-reactive dye composites at different temperatures. Generally, the region from 600 up to about 1500 cm^{-1} for IR spectrum of untreated alumina reflects both the bulk and the surface. Vibrational frequencies below ~1000 cm^{-1} represent Al–O interactions associated with the absorption bands of AlO_6 octahedrons and AlO_4 tetrahedrons in the range 500–700 and 700–900 cm^{-1}, respectively [Fig. 2A (curve a)] [22, 23]. In addition, the IR spectrum of the same sample exhibits a broad H-bonded OH stretch centred about 3463 cm^{-1} and weaker HOH bending peak at 1650 cm^{-1}. The water is bonded physically and chemically to the alumina surface which has many different crystal planes, edges, or corners [10, 17]. Furthermore, the broad band in the 1430–1380 cm^{-1} region can be attributed to contamination of carbonate species [23]. In the case of IR spectrum of the alumina–RR 120 dye composite at room temperature, the peaks (3566, 3490 and 3438 cm^{-1}) in OH stretching region corresponding to the interaction between water molecules and alumina at room temperature are ascribed to the presence of Al–OH and H–O–H (for H_2O) stretching bands [Fig. 2A (curve b)]. The very small peaks in the 1400–1600 cm^{-1} region and at 783 cm^{-1} can be attributed to the aromatic

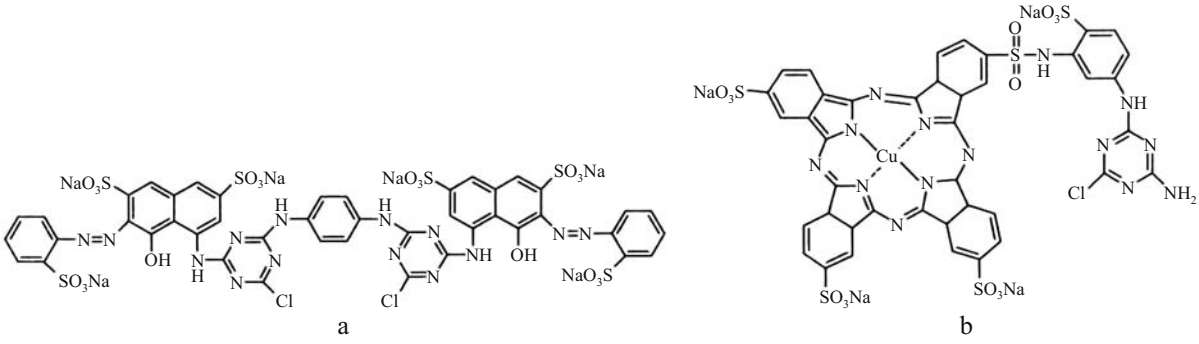

Fig. 1 The molecular structures of a – Reactive Red 120 (RR 120) and b – Reactive Blue 15 (RB 15)

ring vibrations corresponding to C=C stretching, C=C skeleton stretching and C–H out-plane bending. Although the OH stretching band (~3400 cm^{-1}) of phenol group and, the symmetric SO_2 stretching band (1160–1120 cm^{-1}) of the RR 120 dye compound are expected, these bands for this dye–alumina composite are clearly not observed due to overlapping with water bands and the weaker interactions with the surface. However, in the IR spectrum of the same sample, a small shoulder corresponding to the asymmetric SO_2 stretching at 1319 cm^{-1} appeared [Fig. 2A (curve b)]. The similar situation for IR spectrum of the alumina–RB 15 dye composite at room temperature was observed [Fig. 2A (curve f)]. From the strong interactions between water molecules and alumina surface, it is concluded that the water species compete with dye types to form hydrogen bonds with the surface. The bands observed in the low intensities corresponding to functional groups of dye compounds in comparison with water bands point out that the dye species is bound to surface through a water bridge (Figs 3a and b) [14]. This bonding for RR 120 is through its OH group, whereas that of RB 15 is via its NH_2 groups.

The composites obtained by a mechanochemical treatment between the alumina and dye compounds showed stronger surface interactions with respect to water solution. In the IR spectrum of RR 120–alumina complex, the asymmetric and symmetric $S(=O)_2$ stretches at 1324 and 1206 cm^{-1} respectively, the S–O–C stretching band at 1046 cm^{-1}, and the vibrations of aromatic ring within the range 1600–1400 cm^{-1} were clearly seen [Fig. 2B (curve a)]. The surface of RB 15–alumina complex behaved similarly that symmetric $S(=O)_2$ (1191 cm^{-1}) and the S–O–C (1035 cm^{-1}) stretching bands, and the vibrations of aromatic ring were detected [Fig. 2B (curve b)].

Both alumina–dye complexes were heated from room temperature to 350°C stepwise to observe spectral changes. The thermal treatment of the alumina–RR 120 composite at 150°C resulted in the dehydration and decomposition processes as indicated by the weakening of bands in the OH and aromatic ring stretching regions [Fig. 2A (curve b)]. These decreases in the IR band intensities for the alumina–dye complexes in the temperature range 250–350°C were more clearly observed as the decomposition proceeded [Fig. 2A (curves c–e)]. However, the appearance of the small S–O–C stretching peaks in the IR spectra of alumina–RR 120 (~1100 cm^{-1}) and RB 15 (1040 cm^{-1}) composites up to 250°C may be ascribed to the existence of organic residue on the surface after evolution of the water [24]. The IR data recorded after thermal treatment of these composites can be interpreted in terms of the fragments generated

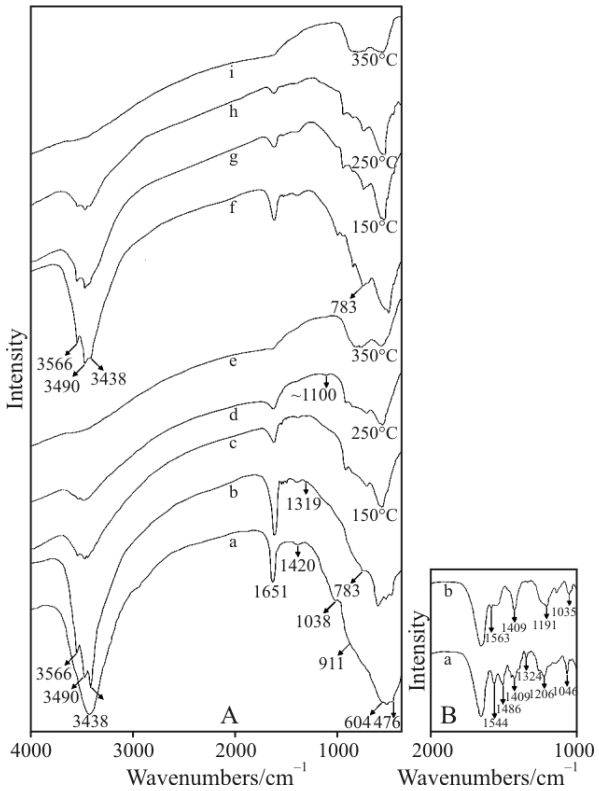

Fig. 2 IR spectra of A – a – untreated-alumina, b–e – alumina–RR 120 dye composites, f–i – alumina–RB 15 dye composites heated in the interval temperature 25–350°C, respectively and B – a – alumina–RR 120 dye composite and b – alumina–RB 15 dye composite obtained by mechanochemical treatment

by breaking of dye-water bridge species interacted directly with the alumina surface.

The thermal behaviour of the alumina is shown in comparison with alumina-dye complexes (Figs 4a–c) together with the mass losses obtained TG curves in each stage in Table 1. The endothermic peak in the temperature range 26–417°C on the DTA curve of the alumina corresponds to the removal of moisture and surface adsorbed water having mass loss by 12.36 [8, 9]. In addition, the mass loss by 1.05% at 417–731°C represents the formation of δ and θ phases [9]. The table data also exhibit that the need for energy to form these phases in comparison with the evolution of water is higher due to lattice changes [10]. The mass loss occurred by heating the alumina (γ) up to ~1100°C illustrates the formation of α-Al_2O_3 [13]. Although some of the dye molecules at lower temperatures are removed from the alumina surface together with water molecules, the additional endothermic peaks at 237°C (RB 15) and ~249°C (RR 120), and the bigger total mass losses for the alumina–dye composites exhibit decomposition of the dye species retained by the same surface. Furthermore, the mass losses on TG curves during thermal treatment of the same samples up to

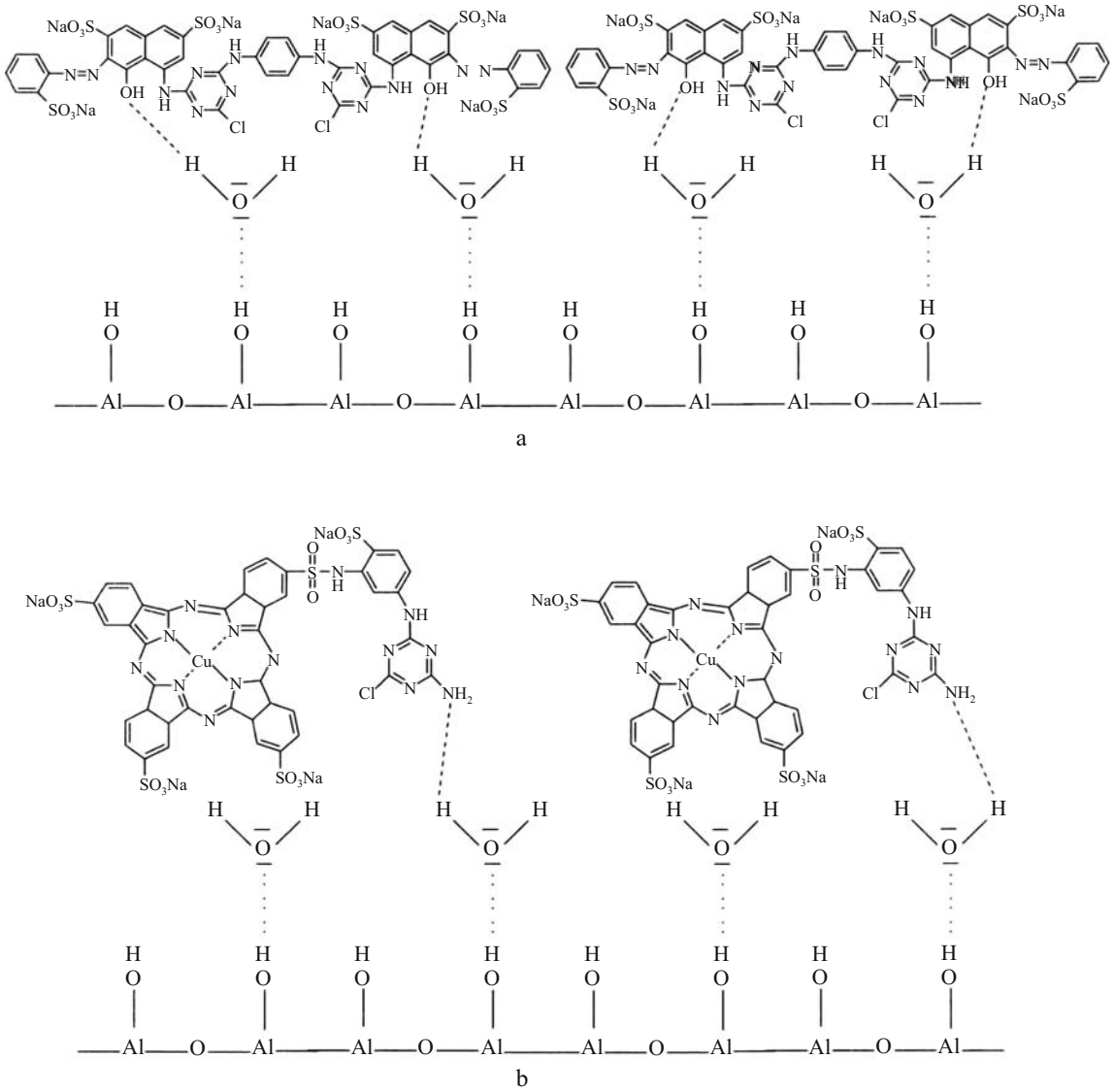

Fig. 3 The schematic representation of interaction of a – RR 120 and b – RB 15 dye types on the alumina surface

~800°C were attributed to removal of black residues occurred by decomposition of first adsorbed products [25]. After thermal dehydration, the dye types with low decomposition energy in the range ~200–400°C clearly reveal that the water molecules are bonded strongly to the same surface and compete with these types to accommodate the surface active sites (Table 1). The result also support that the functional groups of bigger dye molecules with respect to water molecules are not completely accessible active sites of the surface due to the steric effect [14, 26]. In addition, thermal treatment also changes the surface properties

Table 1 Thermal analysis data of untreated alumina and alumina–reactive dye composites

Sample	DTG_{max}/ °C	ΔH/ J g^{-1}*	Temperature range/°C**	Mass loss, Δm/ %	Total mass loss, Δm/%
Basic alumina	49	246.67	26–417	12.36	13.41
	572	925.20	417–731	1.05	
Alumina–RR 120 dye composite	48	333.97	25–195	13.35	17.66
	237	6.25	195–322	1.61	
	–	861.87	322–800	2.70	
Alumina–RB 15 dye composite	52	388.31	25–197	12.18	16.58
	237	16.14	197–433	2.00	
	–	915.30	433–800	2.40	

*The decomposition enthalpies (ΔH/J g^{-1}) of each stage were calculated by converting DTA signals to DSC data.
**The temperature ranges were obtained from the DTA curves

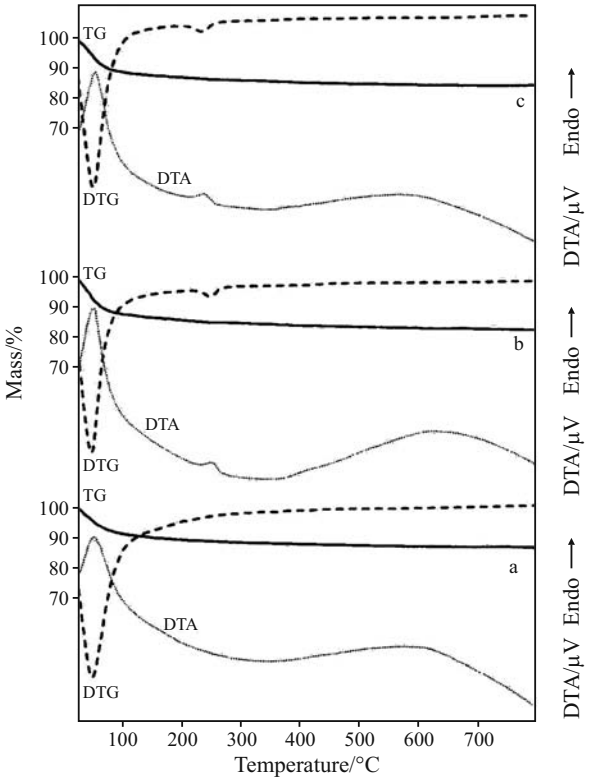

Fig. 4 Thermal analysis curves of a – untreated-alumina, b – alumina–RR 120 dye composite and c – alumina–RB 15 dye composite

of Al_2O_3 depending on the surface functional groups [10, 27]. In air at room temperature, the water retention on the alumina surface can generate the OH groups chemically bonded to the surface and these groups may form a hydrogen bond with another polar water molecule (Figs 5a and b) [8, 12]. Although, such groups impart weakly acidic properties to the surface, the bridge bonded oxygen sites occurred by heating the alumina surface demonstrate mainly Lewis basic character (Fig. 5c) [8]. Finally, the dye molecules at low temperature are bonded to the surface through a water bridge whereas the functional groups of residue products formed by decomposition of the same molecules at high temperature interact directly to the surface with the bridge bonded oxygen site.

The comparison of X-ray diffraction patterns of the alumina and alumina-dye composites at room temperature and in the temperature range 150–350°C are given

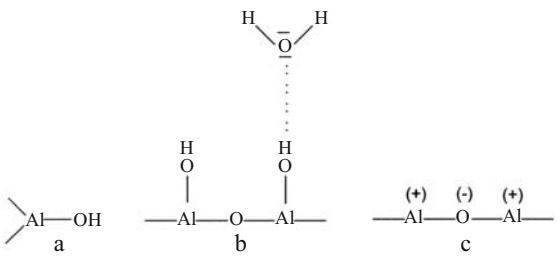

Fig. 5 The surface functional groups in alumina material

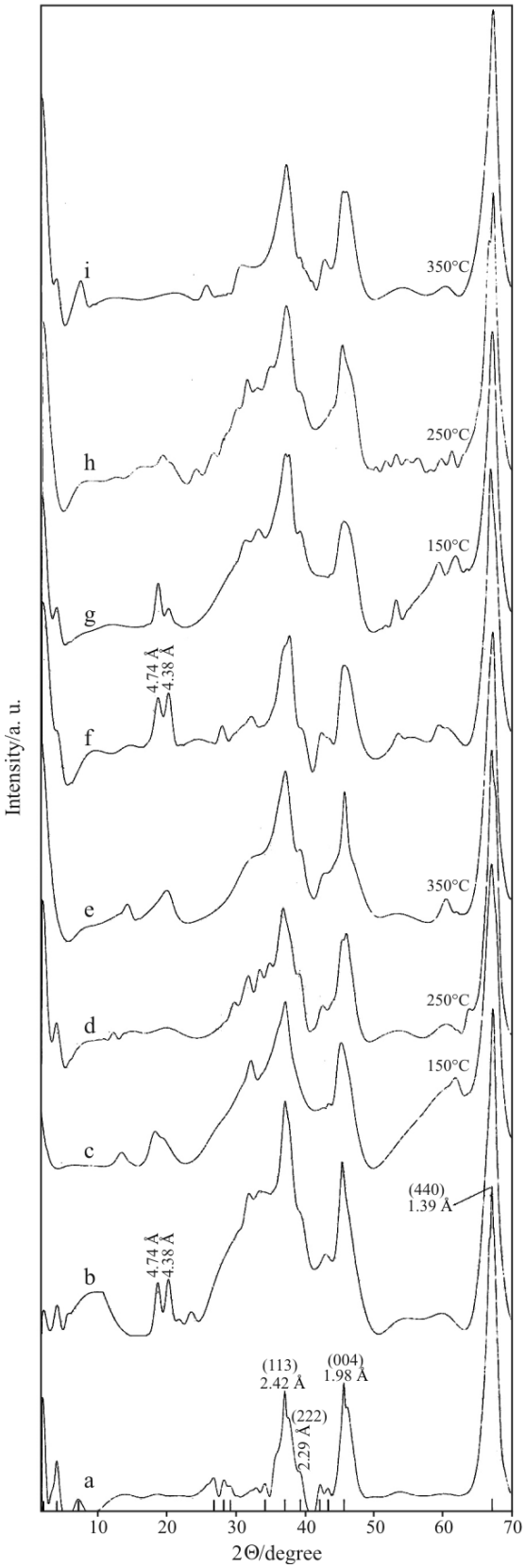

Fig. 6 XRD spectra of a – untreated-alumina, b–e – alumina–RR 120 dye composites, f–i – alumina–RB 15 dye composites heated in the interval temperature 25–350°C, respectively

in Figs 6a–i. The alumina is characterized by strong reflections at about 37.12, 45.68 and 67.04° (2θ) corresponding to d (113), (004) and (440) values about 2.42, 1.98 and 1.39 Å, respectively, a weak reflection at about 39.36° 2θ (d_{222}) and several very weak reflections [9, 28] (Fig. 6a). However, the new X-ray powder diffraction peaks for both alumina–dye complexes at about 18.70 and 20.24° (2θ) appeared indicating the presence of the dye molecules on the surface (Figs 6b and f). In addition, after the thermal treatment in the temperature range 150–350°C, XRD spectra of these composites demonstrated that the intensities of these new bands decreased as a result of the removal of surface types. Nevertheless, the existence of these peaks up to temperatures higher than 150°C can be ascribed to the formation of black residue corresponding to the decomposition of the dye species on the surface at lower temperatures.

Conclusions

The spectroscopic properties of the alumina–dye composites prepared from water solutions were investigated by using X-ray diffraction (XRD), thermal analysis (DTA, TG and DTG) and Fourier transform infrared spectroscopy (FTIR) techniques. The spectrophotometric data of these complexes revealed that the dye species were bonded through the water bridges to alumina surface at room temperatures. Although, the very small IR peaks in the ring region for these composites were observed, the mechanochemical adsorption resulted in stronger interaction indicated by the appearance of asymmetric and symmetric SO_2 stretching bands. When these composite samples were heated in the temperature range 150–350°C, the decreases in the intensities of the IR and XRD peaks implied the removal of dye molecules following breaking of water bridges. However, the presence of these peaks up to high temperatures pointed out the formation of black residue on the surface. The endothermic peaks over 200°C and the bigger total mass losses for the alumina-dye composites also confirmed these results.

Acknowledgements

The financial support of the Research Foundation of Ondokuz Mayis University under the Project number F338 is gratefully acknowledged.

References

1 T. M. Ulyanova, I. I. Basalyga, E. S. Paemurd and N. P. Krut'ko, Mech. Compos. Mater., 38 (2002) 163.
2 G. R. Yurchenko, A. K. Matkovsky, A. P. Shimansky and A. A. Chuiko, J. Therm. Anal. Cal., 62 (2000) 469.
3 S. Goldberg and R. A. Glaubig, Soil Sci. Soc. Am. J., 52 (1988) 87.
4 D. Sternik, P. Staszczuk, J. Sobieszek, M. Planda-Czyz and S. Wasak, J. Therm. Anal. Cal., 86 (2006) 77.
5 W. H. J. Stork and G. T. Pott, J. Phys. Chem., 78 (1974) 2496.
6 M. Planda and P. Staszczuk, J. Therm. Anal. Cal., 62 (2000) 561.
7 E. A. Sergeeva, T. P. Safiullina, O. P. Shmakova, I. N. Bakirova and L. A. Zenitova, Russ. J. Appl. Chem., 79 (2006) 1181.
8 A. S. Arico, V. Baglio, A. Di Blasi, P. Creti, P. L. Antonucci and V. Antonucci, Solid State Ionics, 161 (2003) 251.
9 G. Paglia, C. E. Buckley, A. L. Rohl, R. D. Hart, K. Winter, A. J. Studer, B. A. Hunter and J. V. Hana, Chem. Mater., 16 (2004) 220.
10 J. B. Peri, J. Phys. Chem., 69 (1965) 220.
11 T. D. J. Dunstan and R. E. Pincock, J. Org. Chem., 50 (1985) 863.
12 Z. Zhang and Z. Su, Sep. Sci. Technol., 37 (2002) 733.
13 M. Robinson, J. A. Pask and D. W. Fuerstenau, J. Am. Ceram. Soc., 47 (1964) 516.
14 Y. Mao and B. M. Fung, J. Colloid Interface Sci., 191 (1997) 216.
15 Y. Liu, L. Gao, L. Yu and J. Guo, J. Colloid Interface Sci., 227 (2000) 164.
16 G. W. Kabakla and R. M. Pagni, Tetrahedron, 53 (1997) 7999.
17 J. B. Peri, J. Phys. Chem., 69 (1965) 211.
18 M. Haneda, E. Joubert, J. C. Menezo, D. Duprez, J. Barbier, N. Bion, M. Daturi, J. Saussey, J. C. Lavalley and H. Hamada, Phys. Chem. Chem. Phys., 3 (2001) 1366.
19 A. Pourjavadi, B. Soleimanzadeh and G. B. Marandi, React. Funct. Polym., 51 (2002) 49.
20 M. Nakamura, H. Saitoh, Y. Maejima, S. I. Yamagiwa and S. Kaneko, Fresenius' J. Anal. Chem., 335 (1998) 573.
21 D. K. Lee, I. C. Cho, G. S. Lee, S. C. Kim, D. S. Kim and Y. K. Yang, Sep. Sci. Technol., 34 (2004) 43.
22 G. Paglia, C. E. Buckley, T. J. Udovic, A. L. Rohl, F. Jones, C. F. Maitland and J. Connolly, Chem. Mater., 16 (2004) 1914.
23 J. Y. Ying, J. B. Bengizer and H. Gleiter, Phys. Rev. B, 48 (1993) 1830.
24 A. Tabak, B. Afsin, S. F. Aygun and H. Icbudak, J. Therm. Anal. Cal., 81 (2005) 311.
25 A. Tabak, B. Afsin, S. F. Aygun and E. Koksal, J. Therm. Anal. Cal., 87 (2007) 375.
26 A. R. Studart, V. C. Pandolfelli, E. Tervoort and L. J. Gauckler, J. Eur. Ceram. Soc., 23 (2003) 997.
27 I. W. M. Brown, M. E. Bowden, T. Kemmitt and K. J. D. MacKenzie, Curr. Appl. Phys., 6 (2006) 557.
28 X. J. Wang, M. K. Lei, T. Yang and H. Wang, Opt. Mater., 26 (2004) 247.

Received: December, 14, 2007
Accepted: February 19, 2008
OnlineFirst: September 20, 2008

DOI: 10.1007/s10973-007-8914-x